

# Kinetic Simulation of Heating and Collisional Transport in a 3D Tokamak

Andres BUSTOS<sup>1,4</sup>, Francisco CASTEJON<sup>1,4</sup>, Luis A. FERNÁNDEZ<sup>2,4</sup>,  
Victor MARTIN-MAYOR<sup>2,4</sup>, Alfonso TARANCÓN<sup>3,4</sup> and José L. VELASCO<sup>3,4</sup>

<sup>1</sup>Lab. Nac. de Fusión – Asociación Euratom/Ciemat, 28040-Madrid, Spain.

<sup>2</sup>Dep. de Física Teórica I. Universidad Complutense, 28040-Madrid, Spain.

<sup>3</sup>Dep. de Física Teórica. Universidad de Zaragoza, 50009-Zaragoza, Spain.

<sup>4</sup>BIFI: Instituto de Biocomputación y Física de Sistemas Complejos, 50009-Zaragoza, Spain

The microwave plasma heating has a strong influence on collisional transport, experimentally observed both in stellarators and tokamaks. The estimate of the interplay between heating and collisional transport implies solving a 5D kinetic equation. We deal with this problem using a recently developed code (ISDEP: Integrator of Stochastic Differential Equations for Plasmas) in a tokamak with ripple as a test device, introducing the heating effects. In this work we develop a method for a non-linear computation of the time-dependent plasma temperature profile, based on several linear calculations. The influence of heating on the relevant transport parameters, on plasma rotation and on the velocity distribution function is studied.

Keywords: Ion cyclotron resonance heating, ion transport, non-linear simulation.

## 1 Introduction

Transport and heating are usually described as separated processes. The former is customarily solved by fluid equations and the latter, which is considered as a source term of the transport set of equations, is calculated in the framework of kinetic theory. However, there exist several phenomena that show that transport is modified by the heating effects (see e.g. [1, 2]), due to the interplay between microwave plasma heating and transport, and must be estimated solving the 5D kinetic equation (3D in space and 2D in momentum space).

In this work we solve simultaneously the ion transport and heating in the non-linear regime, taking advantage of the equivalence between the linear Fokker Planck (FP) and Langevin equations [4]. As it is well-known, the FP equation is a collective description of the system, i.e. an equation for the distribution function in phase space  $f(t, x)$ . An equivalent form is describing the system with a Langevin equation, which is a Stochastic Differential Equation (SDE) for a single particle, where the variation of  $x_i$ , the phase space coordinate, depends on a deterministic term, proportional to  $dt$ , and on a random term  $dW^i$  that describes a Wiener process [4].

We use ISDEP, a Monte Carlo code that calculates the ion kinetic transport by following the guiding centre orbits in the presence of electric field, including ion-ion [3] and ion-electron collisions [5]. We introduce in the equations a new term that estimates the microscopic quasi-linear wave-particle interaction and was firstly written in Langevin form in [6]. As we deal with ion transport, the heating method that we will consider is direct Ion Cy-

clotron Resonance Heating (ICRH), in the range of second harmonic of ion cyclotron resonance frequency, which is based on launching resonant electromagnetic waves from the edge of the confined plasma. In our case, the randomness represented by the Wiener processes of the interaction is related to the collisions with the background plasma and with the random relative phase between particles gyromotion and waves. In this work, we do not introduce any kind of turbulent transport yet. The wave-particle interaction is formally the same as in the ECRH case, i.e., it can be considered as a resonant diffusion in momentum space. We will include the nonlinear evolution of the background temperature using a self consistent method, updating the temperature at each step.

We choose a tokamak device with ripple instead of a complex device, since we are interested in studying the influence of the heating on transport rather than on the confinement properties of a given magnetic configuration. This application shows the usability of stellarator tools in 3D problems that appear in tokamaks.

## 2 Modeling of collisional transport and heating.

### 2.1 The Langevin Equations for the system

The dynamics of the test particles is given by a set of Langevin equations. This includes several physical features and approximations. We study the evolution of the guiding center position, the velocity square and the pitch:  $x^j = (\vec{r}_{gc}, v^2, \lambda)$ ,  $\lambda = v_{\parallel}/v$ . We also consider Coulombian collisions with the background using the Boozer-Kuo Pe-

author's e-mail: andres.debustos@ciemat.es

traviv collision operator.

The quasilinear wave-particle interaction used in this work is a resonant process in phase space. The resonant condition is satisfied with very small probability, but the influence on  $(v^2, \lambda)$  is very strong. We take a Gaussian deposition profile centered at the magnetic axis. As we will see, the final result is a global increase of the energy.

Schematically, the equations we are solving are:

$$d\vec{r}_{gc} = \vec{v}^{gc}(x) dt, \quad (1)$$

$$dv^2 = \left( F_{v^2}^{gc}(x) + F_{v^2}^{coll}(x) + F_{v^2}^{ICH}(x) \right) dt + G_{v^2}(x) \circ dW^{v^2} + G_{vA}(x) \circ dW^A + G_{vB}(x) \circ dW^B, \quad (2)$$

$$d\lambda = \left( F_{\lambda}^{gc}(x) + F_{\lambda}^{coll}(x) + F_{\lambda}^{ICH}(x) \right) dt + G_{\lambda}(x) \circ dW^{\lambda} + G_{\lambda A}(x) \circ dW^A + G_{\lambda B}(x) \circ dW^B. \quad (3)$$

$$d\lambda = \left( F_{\lambda}^{gc}(x) + F_{\lambda}^{coll}(x) + F_{\lambda}^{ICH}(x) \right) dt + G_{\lambda}(x) \circ dW^{\lambda} + G_{\lambda A}(x) \circ dW^A + G_{\lambda B}(x) \circ dW^B. \quad (4)$$

$$+ G_{\lambda B}(x) \circ dW^B. \quad (5)$$

The Wiener process is an independent increment stochastic process (Gaussian distributed) such that:

$$dW^j(0) = 0, \quad \langle dW^j(t) \rangle = 0, \quad (6)$$

$$\langle dW^j(t) dW^k(t) \rangle = \delta^{jk} dt. \quad (7)$$

This process introduces diffusion phenomena in the system evolution. Using Eqs. (1), (3) and (5) we can follow particle trajectories in the confined plasma, affected by electromagnetic fields using the guiding centre approximation:  $\vec{v}^{gc}$ ,  $F_{v^2}^{gc}$  and  $F_{\lambda}^{gc}$  [7] and collisions with other particles via the Boozer operator:  $F_{v^2}^{coll}$ ,  $F_{\lambda}^{coll}$ ,  $G_{v^2}$  and  $G_{\lambda}$  [8]. The functions  $F_{v^2}^{ICH}$ ,  $F_{\lambda}^{ICH}$ ,  $G_{vA}$ ,  $G_{vB}$ ,  $G_{\lambda A}$  and  $G_{\lambda B}$  can be found in [6], although some misprints have been corrected. Even though the work in [6] was developed for ECRH, we take this model for 2<sup>nd</sup> harmonic of ICRH. The symbol “ $\circ$ ” indicates that we are using Stratonovich algebra for the SDE system [4].

The Monte Carlo method is used to integrate a large number of independent trajectories and calculate the main confinement properties as the average energy, particle and heat fluxes, confinement time, etc. One of the main advantages of following independent trajectories is that the simulations scale perfectly in massive parallel clusters. In fact, all the calculations presented in this work have been done using grid computing techniques, see e.g. [9].

## 2.2 Introduction of non linear effects

Linearizing the Boltzmann equation is equivalent to study the test particles keeping fixed the background plasma. This makes impossible the study of heating effects during plasma evolution because no temperature rising will be observed despite the fast ions will transfer their energy to the background. To overcome this limitation while keeping the benefits of the equivalence between the FP and the Langevin approach, we allow time dependent temperature profiles:  $T(\rho, t)$ , which we shall fix self-consistently by

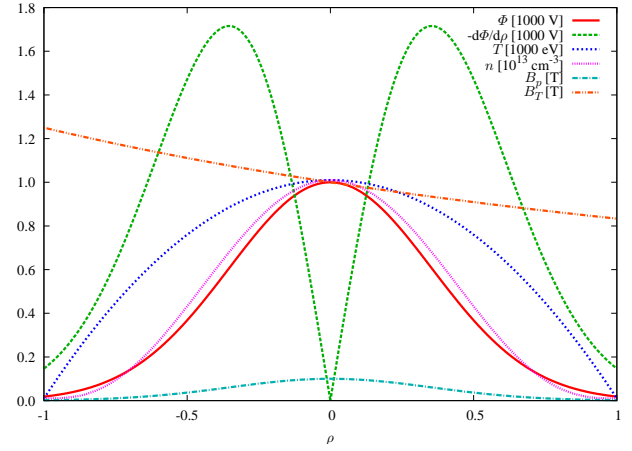


Fig. 1 1D profiles: electrostatic potential ( $\Phi$ ) and its derivative, proportional to the electric field ( $d\Phi/d\rho$ ), temperature ( $T$ ), density ( $n$ ) and poloidal ( $B_p$ ) and toroidal ( $B_T$ ) magnetic fields. In this picture, the values with  $\rho < 0$  correspond the high magnetic field side of the device while  $\rho > 0$  refers to the low field side. All the profiles except  $B_T$  are symmetric in the poloidal angle.

identifying the time evolution of the temperature of the test particles with that of the field particles [5]. Note that time dependent profiles are allowed in a linear FP equation, the iterative method is the key point to introduce non linearities, as will be explained below. In this work we keep constant the background density, assuming that the sources are able to supplement the particle losses.

We use as temperature profile the average kinetic energy in an interval of  $\Delta\rho = 0.1$  centered in  $\rho$  at a time  $t$ :  $v^2(\rho, t)$ . Let  $q_i$  be the quotient of the average kinetic energy in the  $i$ -th iteration with ICH and the energy without ICH. Then, in the iteration  $i + 1$  we take as temperature the initial profile multiplied by  $q_i$ :

$$q_i(\rho, t) = \frac{v_i^2(\rho, t)}{v^2(\rho, t)}, \quad T_{i+1}(\rho, t) = T_0(\rho) q_i(\rho, t). \quad (8)$$

We stop iterating when  $T_{i+1}(\rho, t) = T_i(\rho, t)$  within errors, which is our self-consistent profile.

## 2.3 The tokamak model

In our test device, the plasma is a circular torus with major radius  $R_0 = 1$  m and minor radius  $a = 0.2$  m. The main magnetic field ( $B_0 = 1$  T) as well as a small ripple, ( $\sim 0.01 B_0$ ) is created by 32 toroidal coils. The expression for the rippled magnetic field is obtained from [10]. The ripple does not modify the toroidal magnetic flux in an appreciable way ( $\sim 0.01\%$ , estimated by numerical integration), so we can take the usual expression  $\rho = r/a$ . ICH microwaves are launched by two antennae located in opposite angles of the torus. We plot the shape of the main profiles in Fig. 1.

### 3 Numerical results

We use a *Kloeden-Pierson* algorithm [4] for solving our SDE system. It is similar to a second order Runge Kutta method for a given SDE for  $X(t)$ :

$$dX^i = F^i(X, t) dt + G_j^i(X, t) \circ dW^j, \quad (9)$$

$$X_{n+1}^i = X_n^i + \frac{\delta}{2} (F^i(X_n) + F^i(X_p)) + \frac{1}{2} (G_j^i(X_n) + G_j^i(X_p)) \Delta W^j, \quad (10)$$

$$X_p^i = X_n^i + F^i(X_n) \delta + G_k^i(X_n) \Delta W^k. \quad (11)$$

This method converges weakly (for the averages, see [4]) with order  $\delta^2$  ( $\delta = t_{n+1} - t_n$ ) for a 1D multiplicative noise. Unfortunately, we are dealing with 4D multiplicative noises and we find convergence up to order  $\delta$  (specially in the ICH case).

We perform several linear simulations updating the temperature according to (8) and we stop iterating when we reach the self-consistent profile in  $v^2$  (Fig. 3). The main results of this work are the comparison of fluxes, velocities, distribution functions and other relevant quantities between simulations with and without heating. In Fig. 2 we show the time evolution of several plasma features in both cases: persistence  $\mathcal{P}$  (defined as the fraction of surviving particles), effective radius and kinetic and total energy. It can be seen that the persistence of particles falls faster in the case of ICH. This is not surprising since the average energy is increased and so does the outward flux. We calculate the confinement times fitting  $\mathcal{P}(t)$  to  $e^{-t/\tau}$ . The average radius also increases in the case of ICH for times larger than the typical collision one, showing again the increase of the outward particle flux. The average energy rises for times larger than  $10^{-3}$  s, showing the obvious effect of plasma heating and the typical time scale in which the power absorption is relevant. The change of the average squared velocity is, not surprisingly, very similar to the energy one.

Also we calculate the toroidal and poloidal velocity profiles (Fig. 3). We see that the poloidal velocity does not change because it depends mostly on the  $\vec{E} \times \vec{B}$  drift, and it is not modified in the system. On the other hand,  $v_\phi$  is strongly influenced by ICH, because if  $v^2$  grows while  $v_\theta$  is constant, then  $v_\phi$  increases. This increment, focused on  $\rho \simeq 0$ , is propagated radially via transport processes. The evolution of the particle flux profile is plotted in Fig. 4, which shows that this is always larger in the presence of heating, especially for  $t > 10^{-3}$  s, which is the typical time scale for plasma heating to be relevant. The steady state flux is monotonic, as corresponds to the absence of sources or sinks. The heat flux profile evolution (Fig. 5) is again monotonic in steady state ( $t = 5 \cdot 10^{-2}$  s), but the gradient in the centre of the device is much larger in the case of ICH than in the one without heating, since the heat source is located close to  $\rho = 0$ .

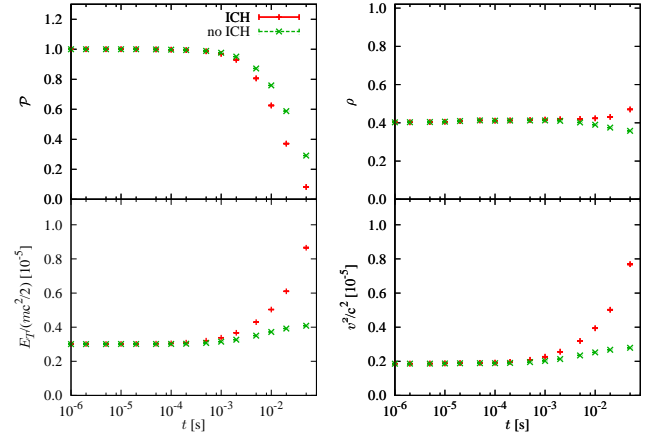


Fig. 2 Evolution (with and without ICH) of the persistence  $\mathcal{P}$  (upper left), average effective radius,  $\rho$  (upper right), total energy  $E_T$  (lower left) and kinetic energy (lower right) in units of  $mc^2/2$ . Confinement times are  $\tau = 0.0387(8)$  s and  $\tau_{\text{ICH}} = 0.0212(9)$  s. We can observe the heating effect for  $t > 10^{-3}$  s.

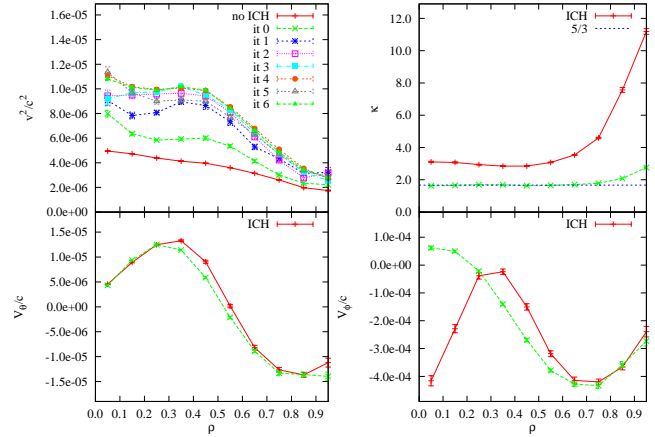


Fig. 3 Iterations of the  $v^2$  profile (upper, left), Binder cumulant (upper, right), poloidal velocity (lower, left) and toroidal velocity (lower, right), measured in  $t = 5 \cdot 10^{-2}$  s.

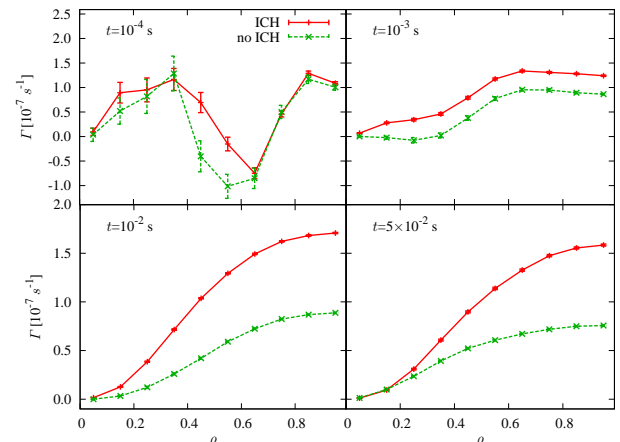


Fig. 4 Particle fluxes.

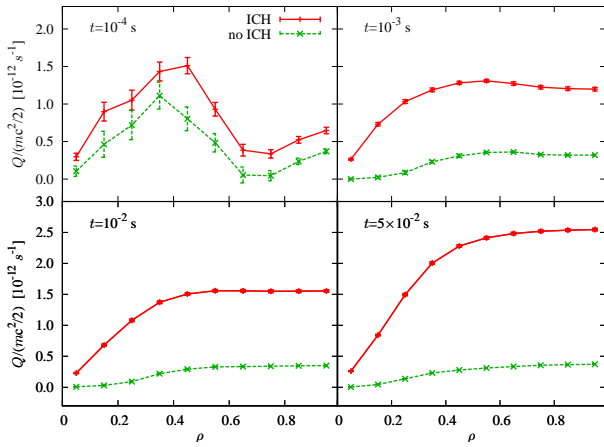


Fig. 5 Heat fluxes.

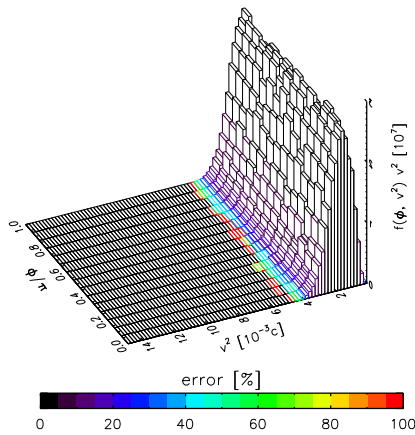


Fig. 6 Velocity probability distribution functions, as a function of the velocity and the toroidal angle without ICH.

We compute and compare the probability distribution function ( $v^2 \cdot f(v, \phi)$ ), in terms of  $v$  and  $\phi$  (Fig. 6). We find that with a small ripple (1%)  $f(v, \phi)$  does not depend on  $\phi$  in any case, which implies that the parallel transport is able to overcome the local heating produced by the antennae as well as the ripple effects. It is clear that the effect of heating tends to make the distribution function wider, rising its tail and creating an important number of suprathermal ions. The Binder cumulant, defined as  $\kappa := \langle v^4 \rangle / \langle v^2 \rangle^2$ , measures deviations from the Maxwellian distribution (Fig 3). In the plasma without ICH, the cumulant is equal to  $5/3$  at every time, except in the outer plasma radius where an increase of fast particles due to the transport is observed. The ICH plasmas show clear effects of heating with a cumulant larger than the Maxwellian value.

## 4 Conclusions

We have estimated for the first time the combined effects of ion collisional transport and heating outside the frame of

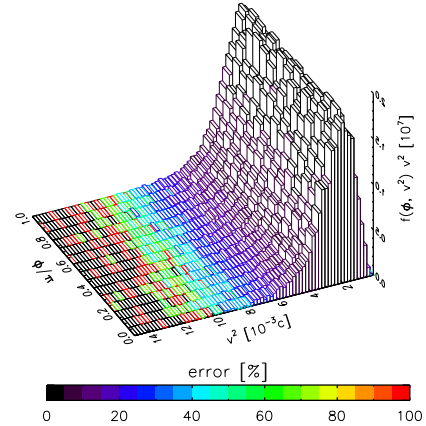


Fig. 7 Velocity probability distribution functions with ICH.

the linear approximation. To do that, we have developed a nonlinear kinetic method based on Langevin equations for transport and quasi linear heating. For the moment, we have considered a non-realistic model for the electric field created by ICRH waves. We modify the background temperature with an iterative method, allowing a real increment of the particle energy. This method makes possible the numerical solution, for any geometry and wave, of the collisional transport in phase space. The only approximations are considering collisional transport in a frozen electrostatic potential and assuming that wave-particle interaction is well described by quasi-linear theory. We have particularized our model to the geometry of a tokamak with ripple, avoiding for the moment the effects of more complex geometries to concentrate ourselves in the heat and transport interplay. This computer code can be easily adapted to another geometries and plasma profiles, like stellarator or ITER geometries.

The authors would like to thank the EGEE Project (EGEE-II INFISO-RI-031688) for enabling grid computing capacity for the calculations performed in this work and T. Happel for his help with some figures.

- [1] F. Castejón *et al.*, Nucl. Fusion **42**,271,(2002).
- [2] M. A. Ochando, F. Medina and the TJ-II Team, Plasma Phys. Control. Fusion **45**, 221 (2003).
- [3] F. Castejón *et al.*, Plasma Phys. Control. Fusion **49** 753, (2007).
- [4] P. E. Kloeden and E. Platen, *Numerical Solutions for Stochastic Differential Equations*, Springer-Verlag, (1992).
- [5] J. L. Velasco *et al.*, Nucl. Fusion **48**, (2008).
- [6] F. Castejón and S. Eguilior, Plasma Phys. Control. Fusion **45**, 159 (2003).
- [7] J. P. Chistiansen and J. W. Connor, Plasma Phys. Control. Fusion **46**, 1537(2004).
- [8] A. H. Boozer and G. Kuo-Petravic, Phys. Fluids **24**(5), 851 (1981).
- [9] F. Castejón *et al.*, Computing and Informatics **27**, 261 (2008).
- [10] A. H. Boozer, Review of Modern Physics **76**, 1071 (2005).